# Measurement of Triple-Differential Inclusive $\nu_\mu$ CC Cross Section at MicroBooNE

London Cooper-Troendle (Yale University)

on behalf of the MicroBooNE Collaboration

NuInt, October 26, 2022

london.cooper-troendle@yale.edu

# Why we are interested in $E_\nu$-dependent Cross Sections

- Inclusive $\nu_\mu$ CC channel, able to tag neutrino flavor, is an important channel for DUNE oscillation measurement
- Kinematics of inclusive $\nu_\mu$ CC defined by 3 degrees of freedom: $\{E_\nu, P_\mu, \theta_\mu\}$
  - $E_\nu$ can be reconstructed with additional $E_{had}$ measurement
- Inclusive $\nu_\mu$ CC in the DUNE energy range consists of several major interaction modes (QE, RES, DIS,...)
  - While final-state particles can be used to separate these modes up to nuclear effects (2p2h, FSI,...), $E_\nu$-dependent cross sections give additional discrimination capabilities

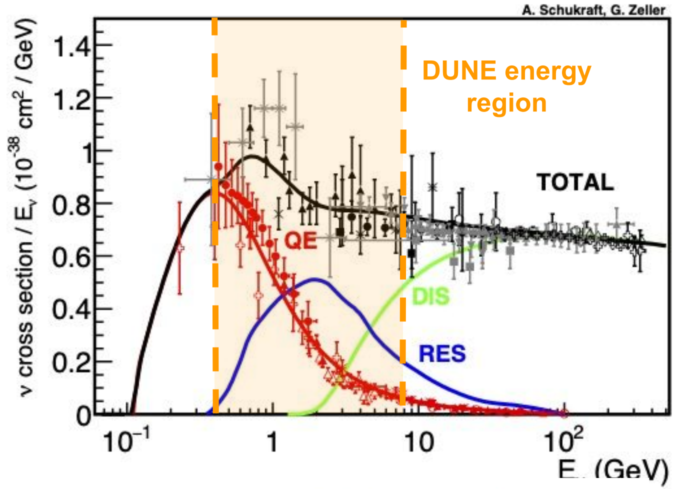


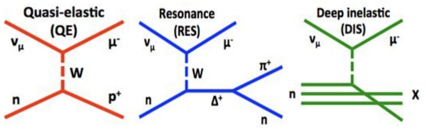


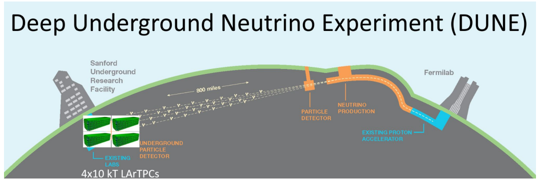


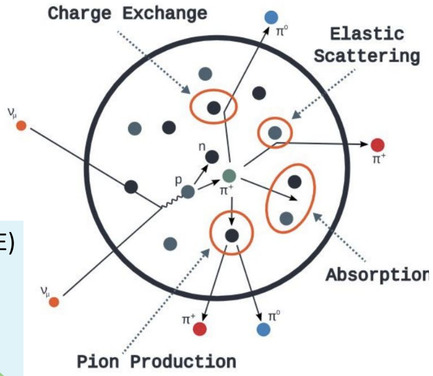

Credit: T. Golan

# The MicroBooNE Experiment

**See Xin Qian's Talk for details**

Detector

Wire Planes

- 85-ton Liquid Argon Time Projection Chamber (LArTPC). Primary goals of:
  - Address MiniBooNE Low-Energy Excess (PRL 128, 241801)
  - R&D for future LArTPC experiments
  - Measurement of $\nu$-Ar cross sections

BNB Flux

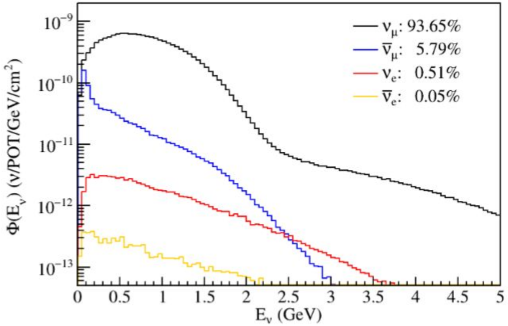


- Situated on-axis on BNB neutrino beam line
  - 0.1-4 GeV, peak at 0.8 GeV

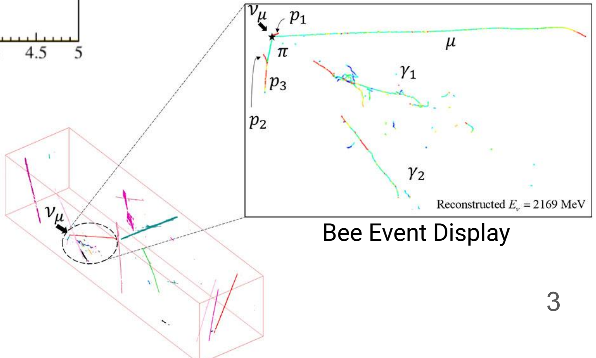


Bee Event Display

- 1.5x$10^{21}$ POT from data taken over 2015-2021
  - 70k inclusive $\nu_\mu$CC events
  - This analysis uses half of the data taken

# $\nu_\mu$ Event Selection

- Begin with 1:20,000 $\nu$:cosmic ray
  - Rejection at ~99.9997% level
- $\nu_\mu$CC selection purity of 92%, efficiency of 68%
- Reconstructed with 3D tomographic imaging, many-to-many flash-charge matching, particle flow hierarchy
  - Select both fully contained (FC) and partially contained (PC) events. FC means that all the deposited charge with a $\nu$ interaction is inside the fiducial volume

Wire-Cell reconstruction: [JINST 16 (2021) 06, P06043]

Cosmic-ray rejection: [Phys. Rev. Applied 15, 064071 (2021)]

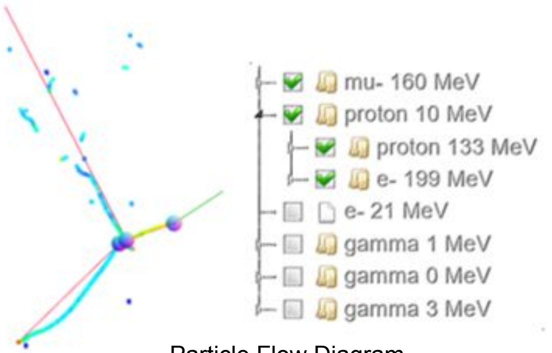


Particle Flow Diagram

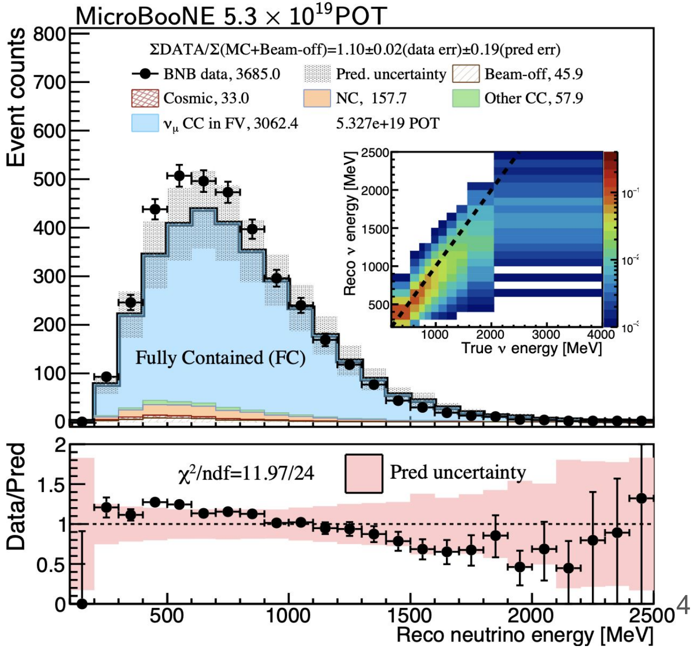

# Energy Reconstruction and Resolutions

- Calorimetry-based energy reconstruction, particle mass and binding energy included
  - **Tracks**: use range, dQ/dx→dE/dx.
    Calibrated and verified by stopped muons & protons
  - **Showers**: sum charge and scale.
    Calibrated by $\pi^0$ invariant mass reconstruction

- Resolutions for fully contained events:
  - $E_\nu$: 20%; $P_\mu$: 10 %; $\theta_\mu$: ~ $5^0$ at forward angles

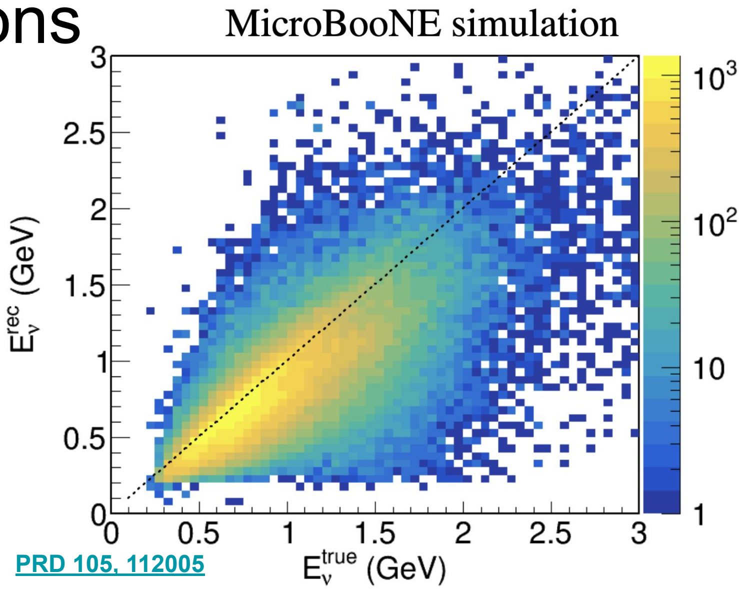


PRD 105, 112005

Fully Contained $\nu_\mu$ CC Events

Binning for $E_\nu$ in [0.2,0.705] GeV

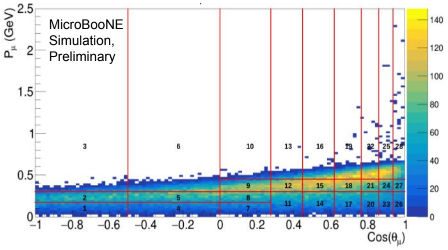


Binning for $E_\nu$ in [0.705,1.05] GeV

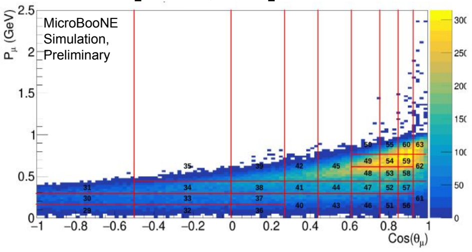


Binning for $E_\nu$ in [1.05,1.57] GeV

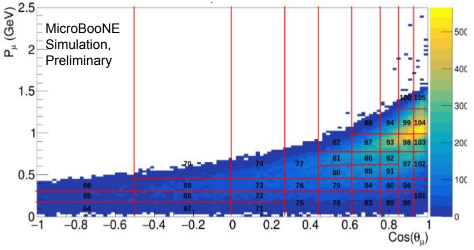


Binning for $E_\nu$ in [1.57,4.0] GeV

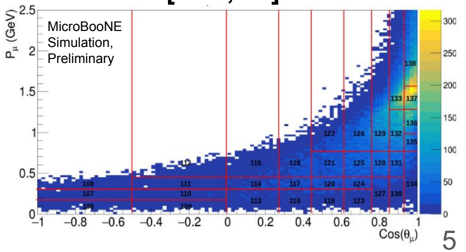


138 analysis bins in total

# Systematic Uncertainties

- **MC statistical uncertainty**: estimated with Poisson likelihood with a Bayesian approach
- **Flux prediction**: MiniBooNE prediction updated to MicroBooNE baseline
  - PRD 79, 072002
- **Cross Section (Xs)**: Modeled using Genie v3.0.6_g18_10a_02_11a tuned to T2K CC0$\pi$ data
  - PRD 105, 072001
- **Detector Systematics**: TPC waveform, light yield, space charge effect, recombination
  - Estimated using bootstrapping (event resampling)
  - Many bins with limited MC events → overestimate uncertainty
    Smoothing used to address this

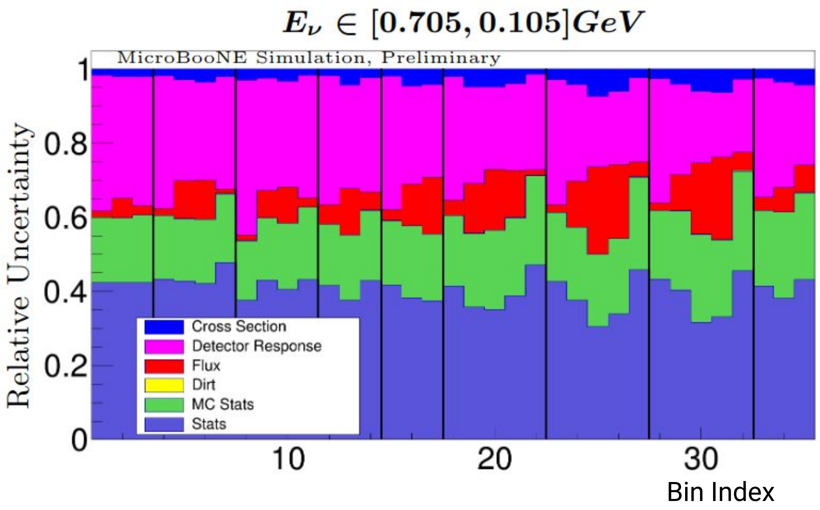


Breakdown of uncertainties fraction within the 2D binning of {$P_\mu$, cos($\theta_\mu$)}. Vertical black bars separate each angle slice, going from backward to forward scattering based on the edges cos($\theta_\mu$) in {-1, -0.5, 0, 0.27, 0.45, 0.62, 0.76, 0.86, 0.94, 1}

Additional (smaller) uncertainties:

- $\nu$ interaction outside cryostat
- GEANT4 model reweighting
- POT from originating proton flux
- Number of target nuclei

# Gaussian Processes Smoothing

- Bayesian approach: uninformed gaussian prior ($\boldsymbol{\mu}$,$\boldsymbol{\Sigma}_T$) updated with input from bootstrapping and kernel function K:
  - Asserts smoothness intuition: nearby bins are correlated
  - Smoothed uncertainties consistent with increased statistics in 1D test
  - Similar formalism as the model validation with conditional covariance

- Factor of 2 reduction in estimated detector systematic uncertainties → improved model prediction for later dedicated validation tests

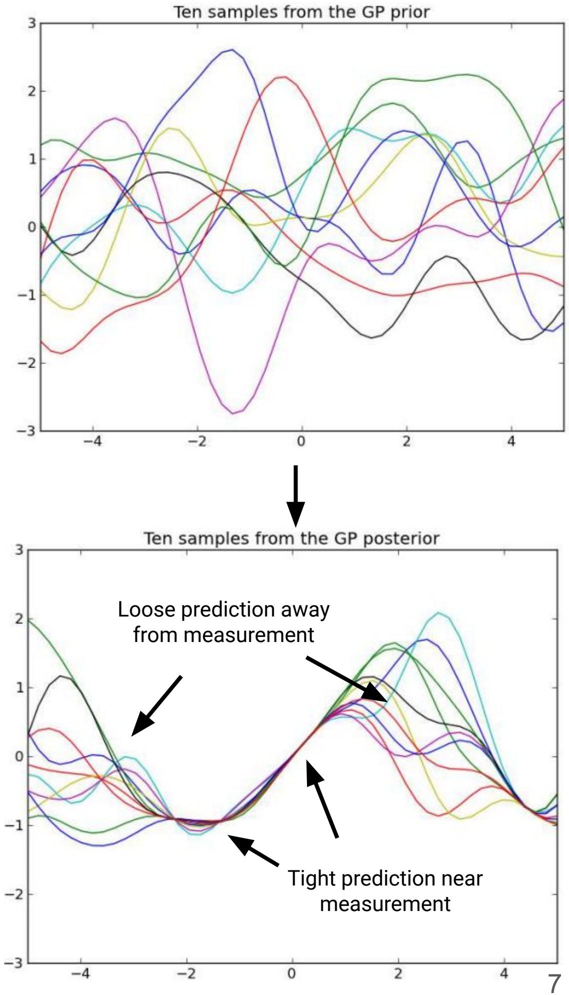

# Previous Single-Differential Energy-Dependent XS

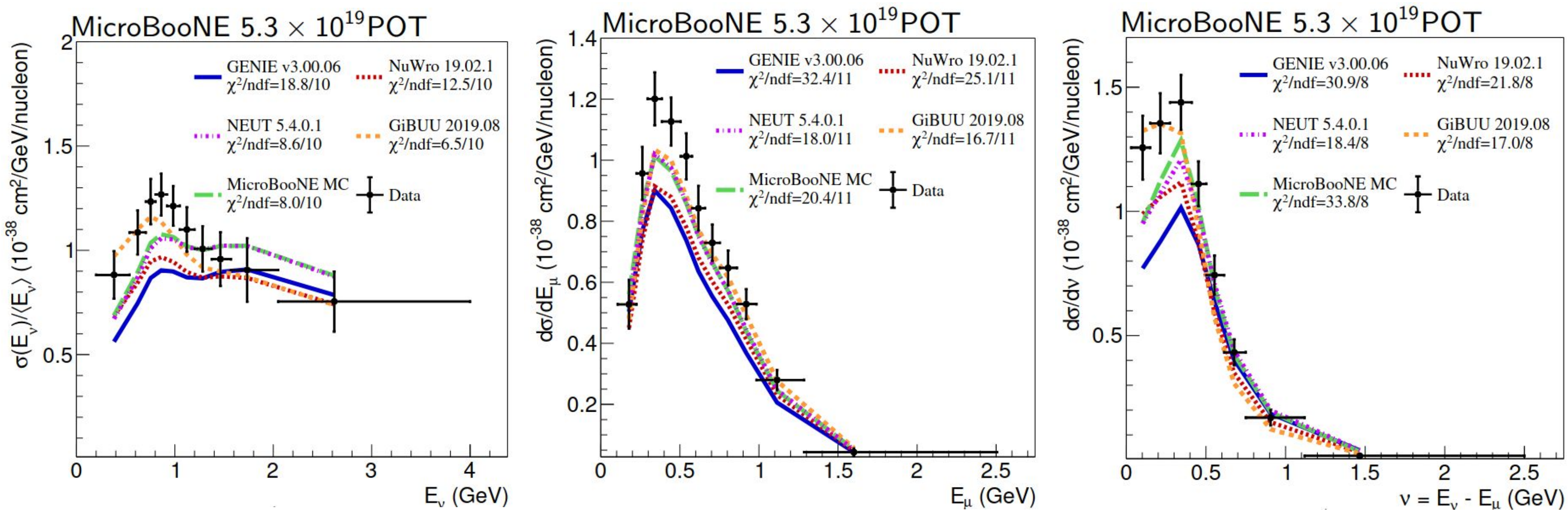


[PRL 128, 151801 (2022)]

Used $5\text{x}10^{19}$ POT data (~3.5% of total data available)

Energy-dependent Xs measurements enabled by the new model validation procedure for $E_\nu^{reco} \rightarrow E_\nu^{true}$ mapping

# Key Analysis Validation Before Unfolding

1. Validate modeling of missing hadronic energy
   a. Novel validation test using conditional constraint
   b. Allows confident unfolding to true $E_{\nu}$

2. Unfold and present results

# Model Validation: $M(E_{had}^{vis})$ vs $\mu(E_{had}^{vis}|E_\nu, E_\mu^{reco})$

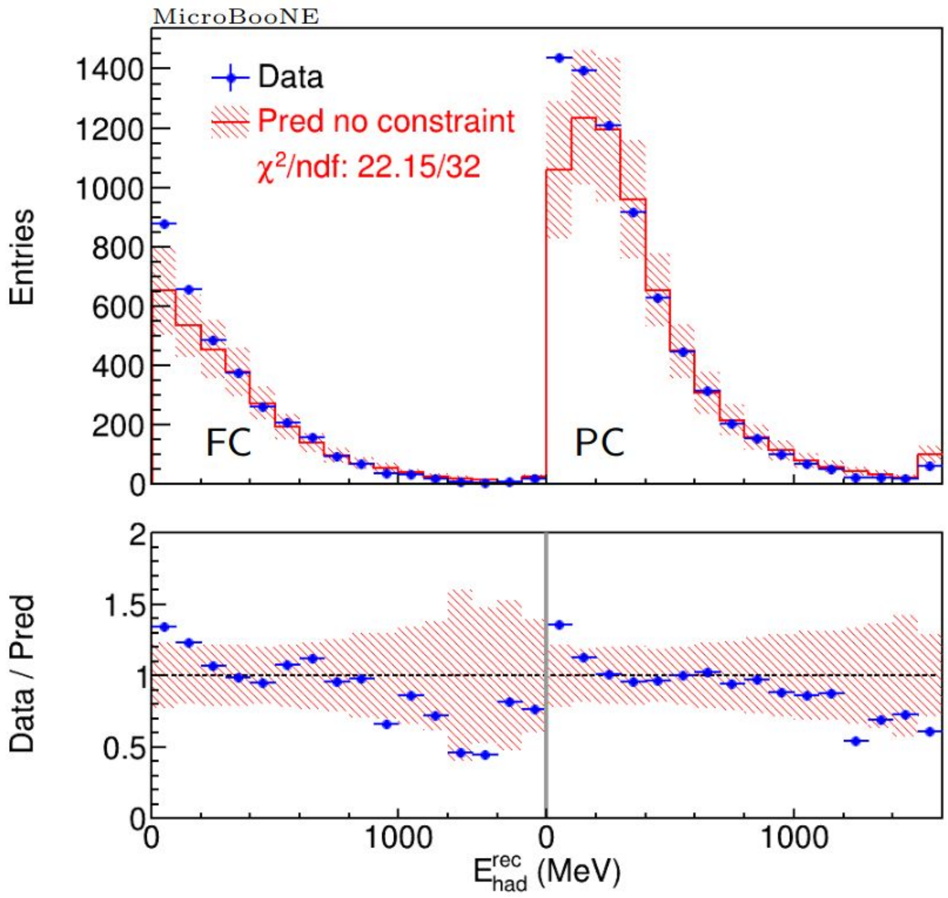


Given by neutrino flux modeling

Muon kinematics measurement

- New method to validate the modeling of neutrino energy
  - Uses LArTPC measurements of lepton kinematics and hadronic energy
- Data/MC goodness of fit tested with $\chi^2$/ndf
  - Muon kinematics used to constrain model prediction of hadronic energy under conditional constraint formalism

# Model Validation: $M(E_{had}^{vis})$ vs $\mu(E_{had}^{vis}|E_{\nu}, E_{\mu}^{reco})$

Given by neutrino flux modeling

Muon kinematics measurement

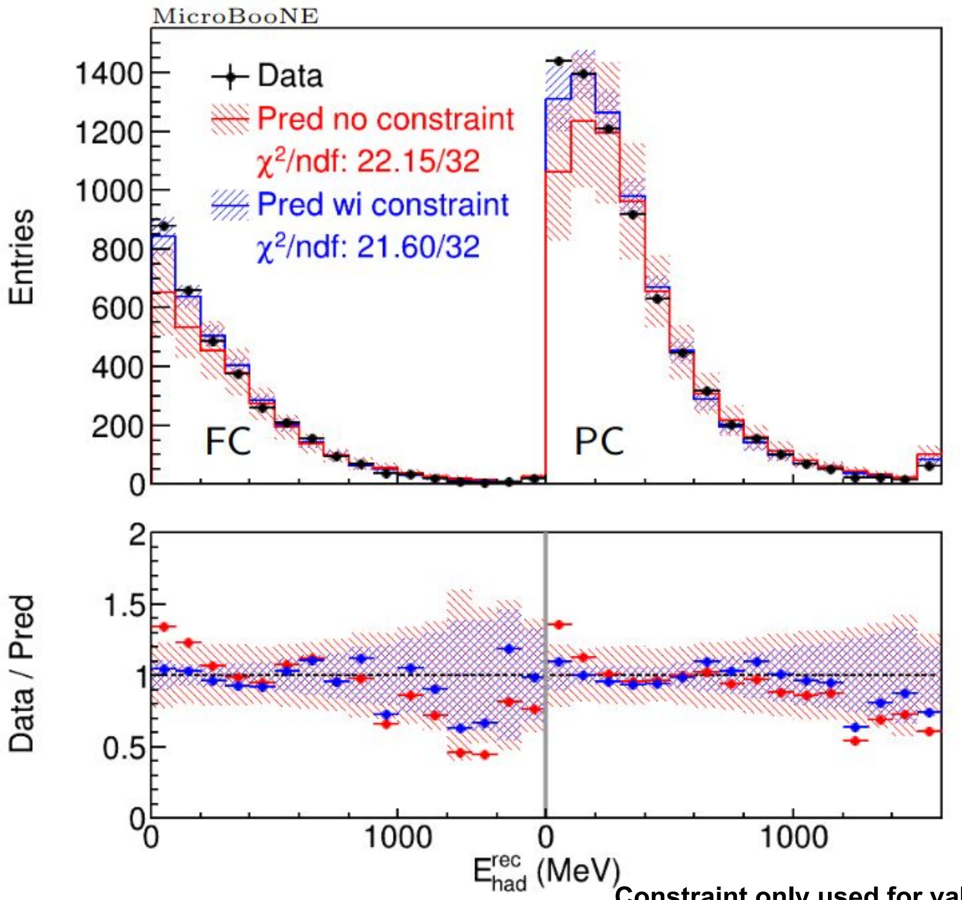


- New method to validate the modeling of neutrino energy
  - Uses LArTPC measurements of lepton kinematics and hadronic energy
- Data/MC goodness of fit tested with $\chi^2$/ndf
  - Muon kinematics used to constrain model prediction of hadronic energy under conditional constraint formalism
- Constraint only used in validation, not unfolding
- Reduced systematic uncertainties in constrained prediction

**Constraint only used for validation, not unfolding**

# Model Validation: $M(E_{had}^{vis})$ vs $\mu(E_{had}^{vis}|E_\nu, E_\mu^{reco})$

Given by neutrino flux modeling

Muon kinematics measurement

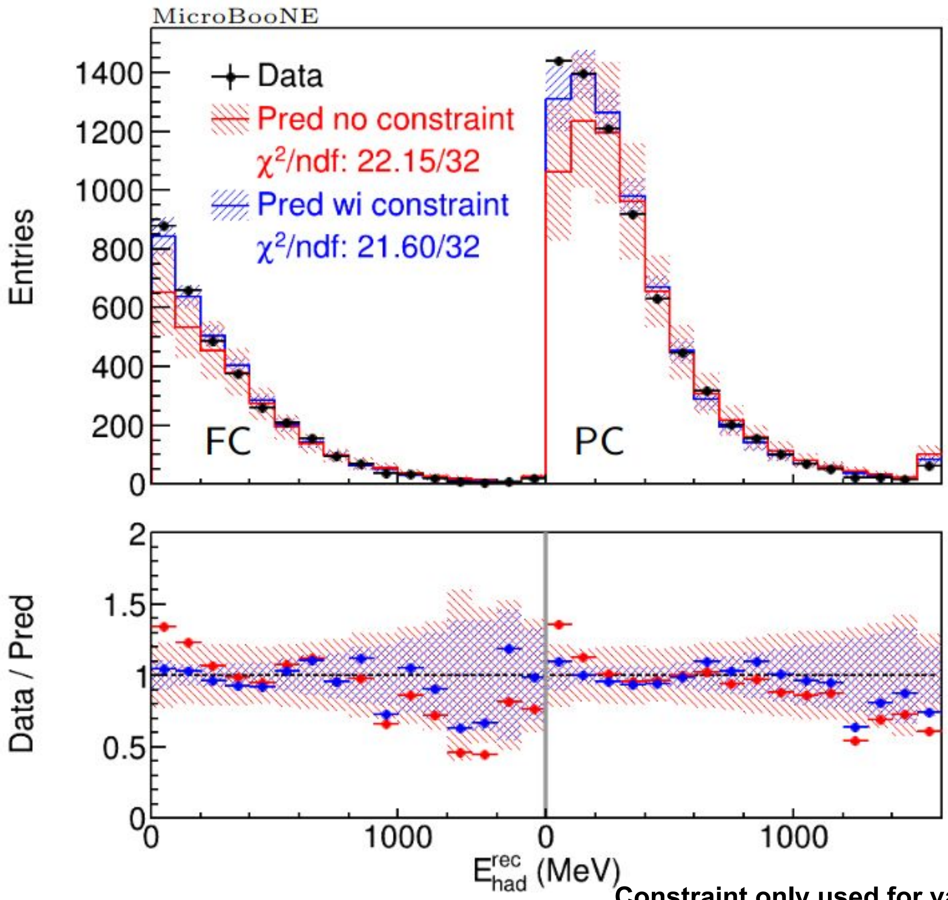


Sensitive to modeling of missing hadronic energy through conservation of energy:

- $E_\nu = E_\mu + E_{had}^{vis} + E_{had}^{missing}$
- $E_\mu$ and $E_{had}^{vis}$ measured directly
- Constrained flux modeling → constrained $E_\nu$ prediction

**Constraint only used for validation, not unfolding**

# Model Validation of Missing Hadronic Energy

- Conditional constraint procedure akin to reweighting based on $P_\mu$ measurement
- QE, RES, DIS predict different $P_\mu$, $E_{had}^{missing}$, and $E_{had}^{vis}$ distributions
  - The constrained prediction of $E_{had}^{vis}$ is sensitive to the modeling of $E_{had}^{missing}$ in each process
- Measurement of constrained $E_{had}^{vis}$ is thus sensitive to the model processes used in $E_{had}^{missing}$ → validation of **the mapping between true and reconstructed $E_\nu$**

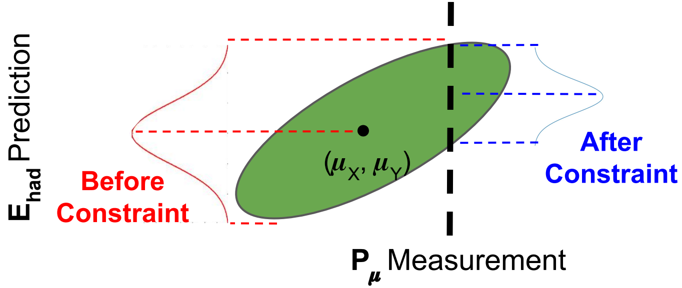


For Illustrative Purposes Only:

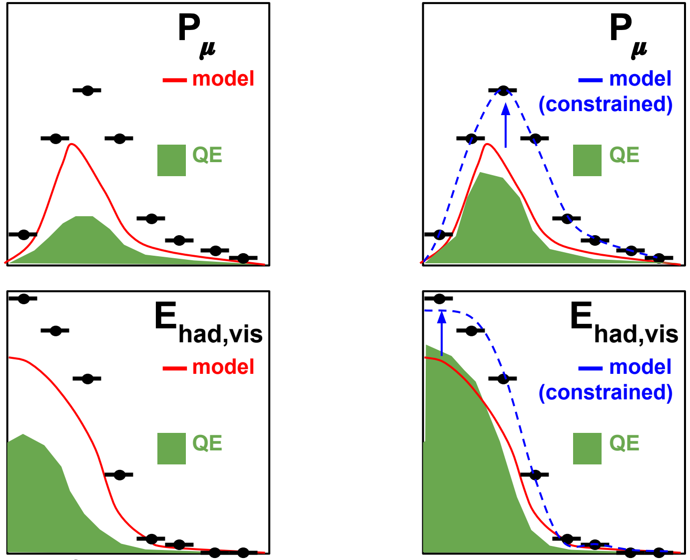


**Constraint only used for validation, not unfolding**

# Testing Model Validation Procedure with Fake Data

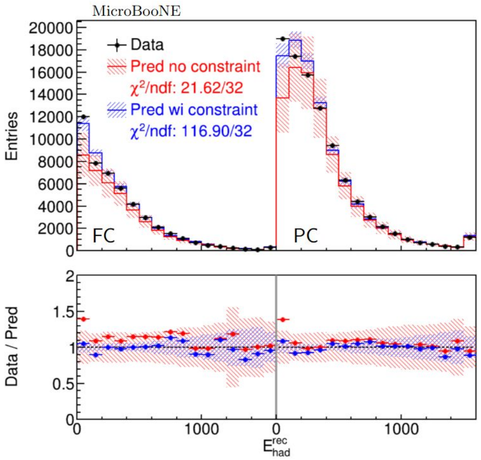


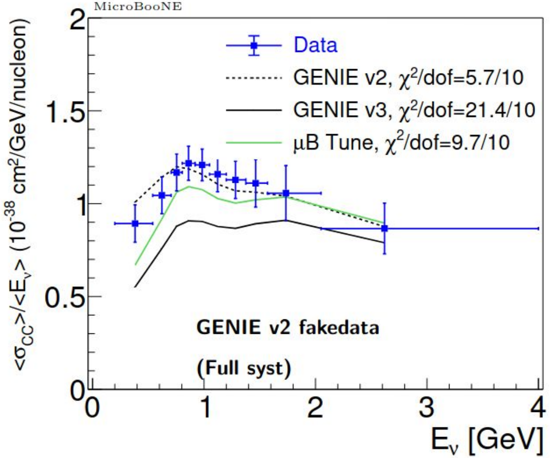


| **Fake Data** | **Model Validation GoF $\chi^2$/ndf (p-value)** | **Unfolded XS w.r.t truth $\chi^2$/ndf (p-value)** |
|---|---|---|
| **Genie v2** | **116.9/32 (1e-10)** | **5.7/10 (.84)** |
| **-30% $E_p$** | **47.1/16 (6.6e-5)** | **5.2/10 (.88)** |

**Constraint only used for validation, not unfolding**

- Fake data generated from scratch with Genie v2 prediction
  - $7.2 \times 10^{20}$ POT exposure used
  - Generated with Poisson distribution, statistically independent
- Constrained model prediction fails validation test → $E_{had}^{missing}$ modeling disagreement
- Unfolded XS consistent with truth
  - Xs extraction is less sensitive to data/model discrepancy than the model validation
  - Consistent with expectation
  - Similar observation in scaled proton energy fake data study, which is non-statistically independent so no bias → $\chi^2$/ndf = 0.

# Model Validation in Single & Multiple Dimensions w. Real Data

## Model Validation in 1D

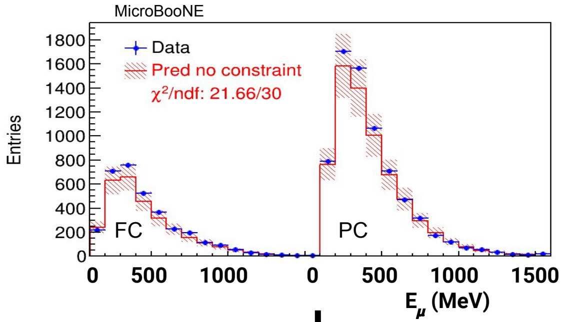


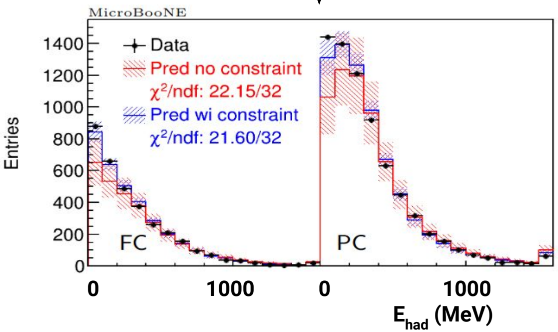


## Model Validation in Multiple Dimensions

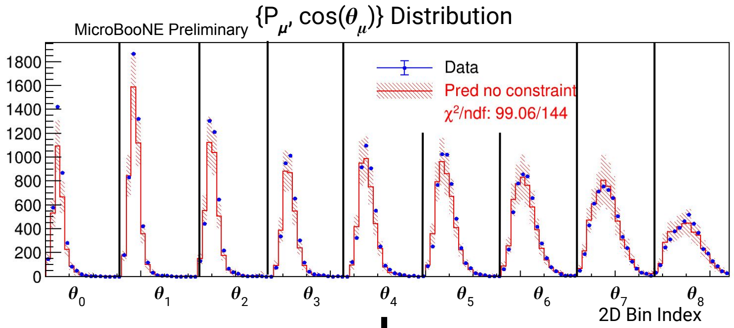


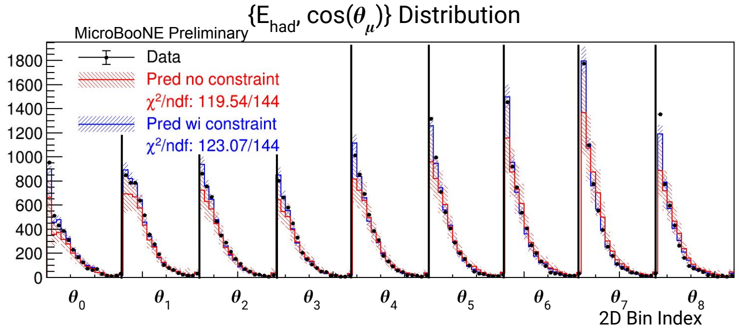


**Constraint only used for validation, not unfolding**

- 2D distribution w/ constraint covers 3D phase space
- Real data passes validation test in 1D and 2D
- Therefore model uncertainty is sufficient to cover potential bias introduced in unfolding

9 angle slices in cos($\theta_\mu$):
{-1, -0.5, 0, 0.27, 0.45, 0.62, 0.76, 0.86, 0.94, 1}
16 $P_\mu$ bins within each angle slice

# Wiener SVD Unfolding and Regularization

*No conditional constraint used in unfolding

- Nominal flux-averaged XS unfolded with Wiener SVD method (JINST 12 P10002)
    - Maximizes the overall signal to noise ratio through the application of the Wiener filter

$$M_i = \sum_j R_{ij} \cdot S_j + B_i$$

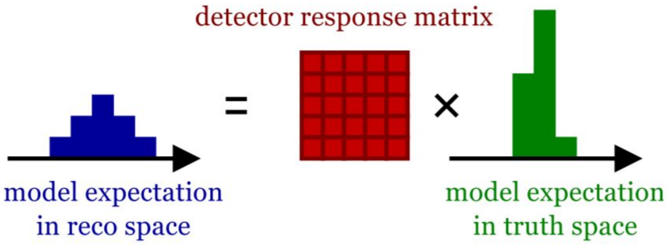


- Regularized using derivatives computed along each of $E_\nu$, $P_\mu$, $\cos(\theta_\mu)$, combined in quadrature:

$$T_{reg}^2 = T_{reg,E\nu}^2 + T_{reg,P\mu}^2 + T_{reg,\cos(\theta)}^2$$

- Bias introduced in regularization and unfolding captured in smearing matrix $A_C$
    - Given with unfolded measurement for bias-free model comparisons

**Test statistic T:**

$$(M-B-R\cdot S)^T \cdot C^{-1} \cdot (M-B-R\cdot S)+T_{reg}$$

# Unfolded Measurement in 3D

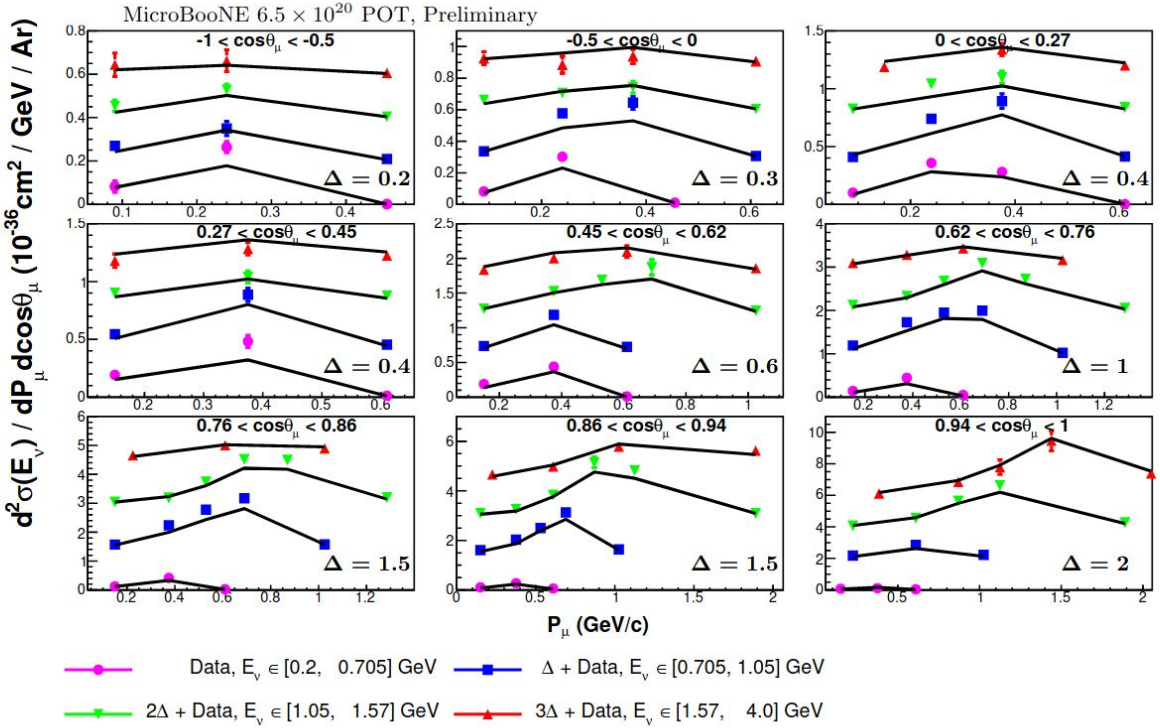


Data plotted against NuWro prediction

$E_\nu$ slices overplot with offset N$\Delta$ for each angle slice

$\Delta$ in same units of $d^2\sigma(E_\nu)/dP_\mu d\cos(\theta_\mu)(10^{-36}cm^2/GeV/Ar)$

| Model Generator | $\chi^2$/ndf |
|---|---|
| Genie v2.12.10 | 740.8/138 |
| Genie v3.0.6 (MicroBooNE Tune) | 313.9/138 |
| Genie v3.0.6 (Untuned) | 309.7/138 |
| GIBUU 2021 | 265.6/138 |
| NEUT v5.4.0.1 | 233.1/138 |
| NuWro v19.02.01 | 200.9/138 |

Descending $\chi^2$/ndf →

3D measurement contains wealth of information → all model central value predictions are now in tension with data

More powerful than 1D measurement, which was consistent with some models

# Example of Usage: Integrated muon momentum for 2D XS

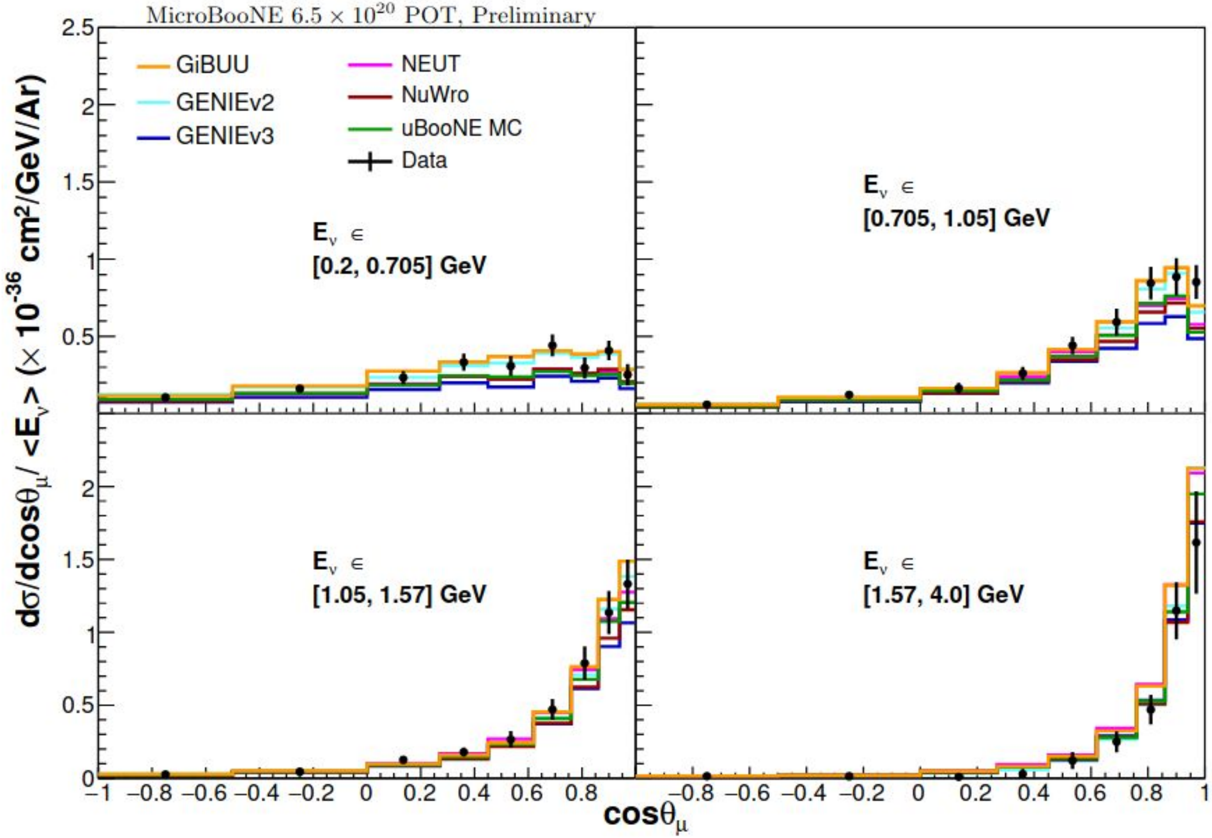


- $\nu$-interaction channels vary over energy range
  - QE fraction 75%→55% from lowest to highest $E_\nu$ bin
- Model performances vary over $E_\nu$
  - **NEUT**'s low overall $\chi^2$ is supported by performance at low energy
  - **NuWro**, **Genie v3** give best prediction at high $E_\nu$, forward angle, where RES fraction is higher
- 3D Xs provides new insights for future model improvement

# Summary and Outlook

- Triple differential cross sections for inclusive $\nu_\mu$CC are measured with high precision in MicroBooNE with LArTPC technology
  - New model validation procedure with conditional covariance allows for a validation of model of missing energy
  - Allows for better model development for DUNE and SBN program

- More results in the future:
  - Twice as much MicroBooNE data available
  - NuMI+BNB combined measurement for improved flux uncertainty
  - Numerous valuable contributions from MicroBooNE:
    40+ publications, tons more in progress on electron neutrinos, proton multiplicity, pion production, NuMI beam measurements, rare searches, methodology, …

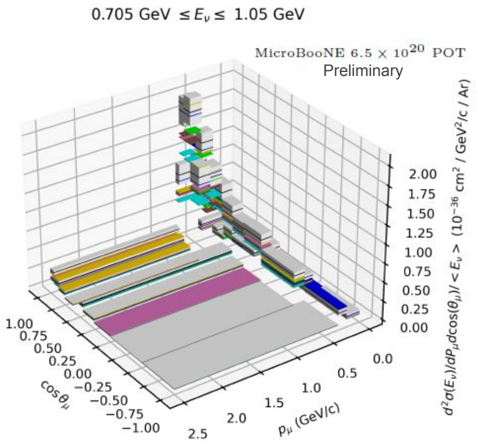


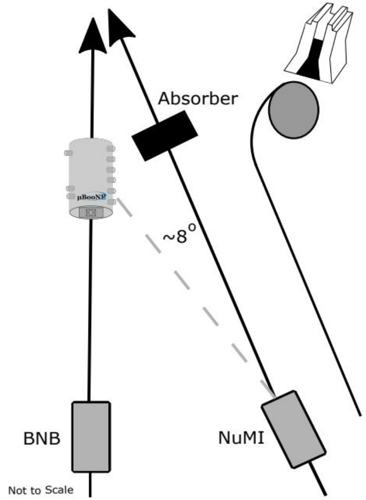

# Backup

# Understanding $\nu$-nucleus Interactions for $\nu$ Oscillations

- Accelerator oscillation experiments aim to definitively answer $\delta_{CP}$, mass hierarchy, etc.
    - DUNE with LArTPC
    - Hyper-K with Water Cherenkov

- Cross section uncertainties or mismodeling may limit the physics reach of these measurements

- Accurate knowledge of the mapping between reconstructed and true $E_\nu$ is very important

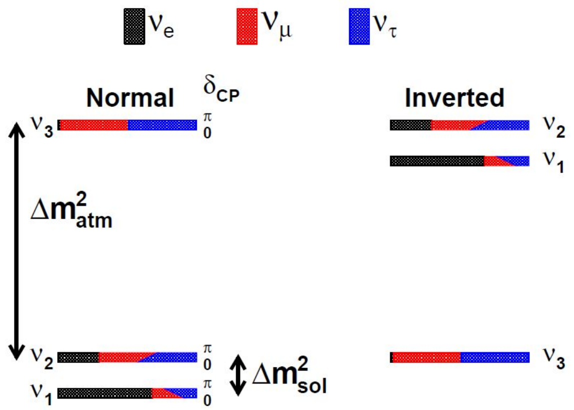


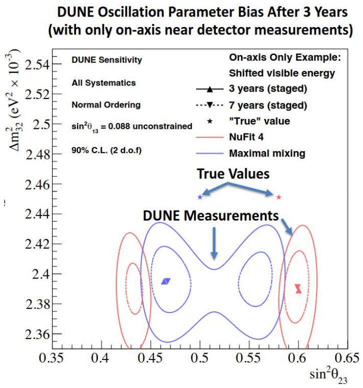


Simulation with 20% of proton energy moved to neutrons

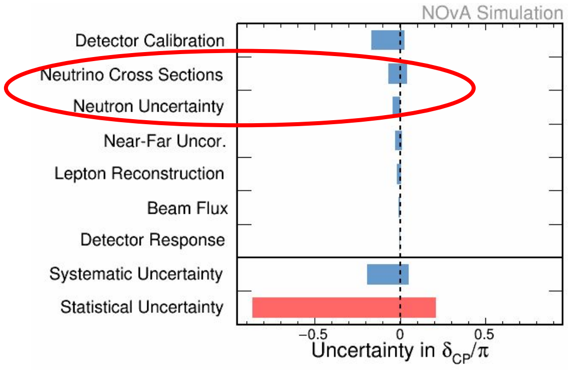


PRD 106, 032004

# Improved TPC Signal Processing, Detector Simulation, and Improved Evaluation of Detector Systematics

- 2D deconvolution algorithm allows to accurately recover the ionization electrons from recorded original signals

- Improved 2D detector simulation, modeling both the long-range induction and the position-dependent effects lead to much better data/MC consistency

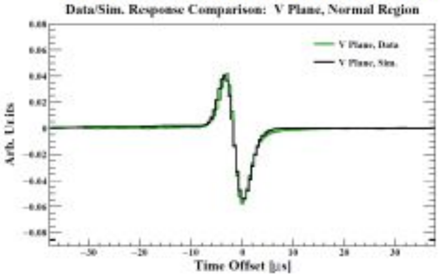


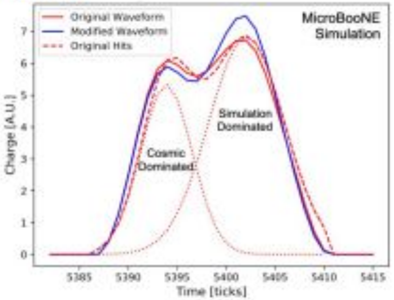


- Improved evaluation of detector systematic uncertainties with changes to detector modeling

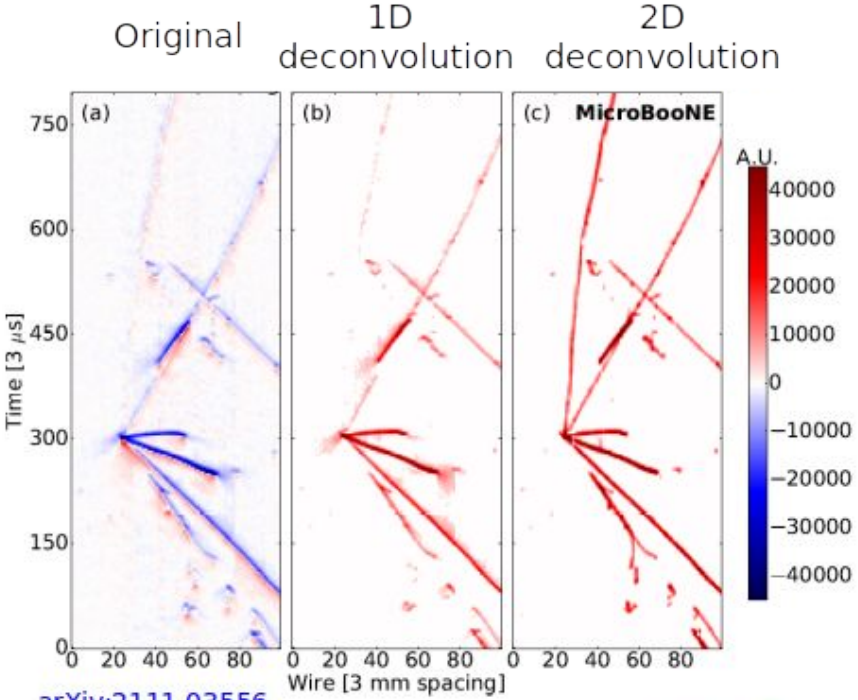


arXiv:2111.03556

JINST 13 P07006/7

# The First **Many-to-Many** Charge-Light Matching

*JINST* **16** P06043

3D imaging, clustering

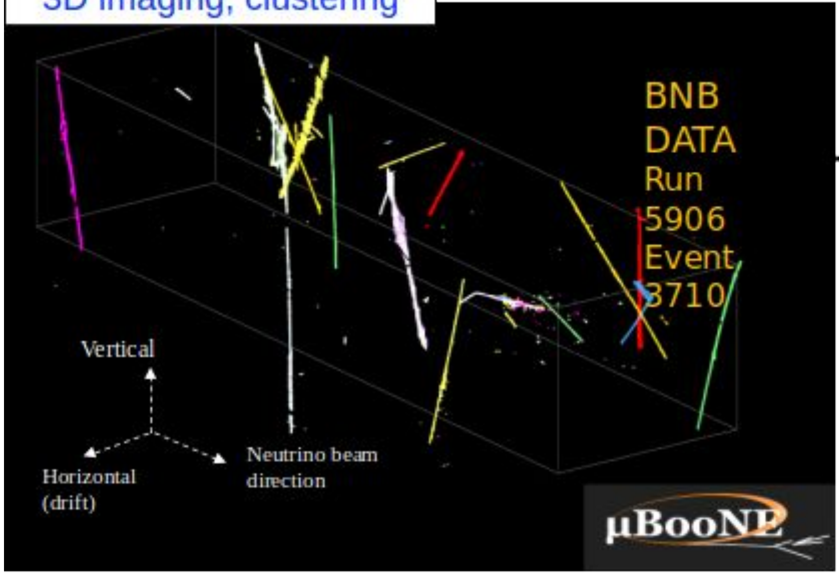


Charge-light matching

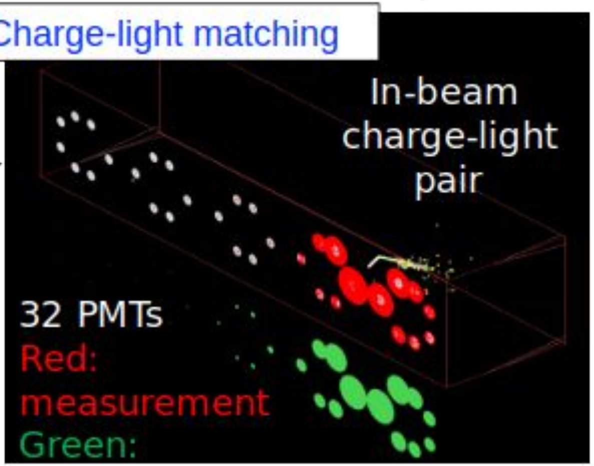


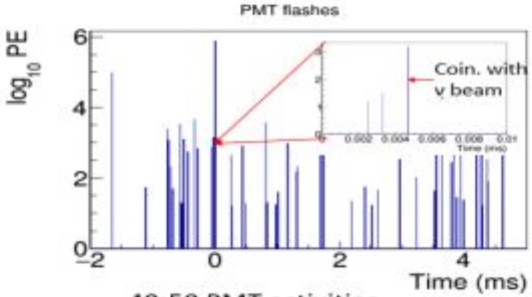


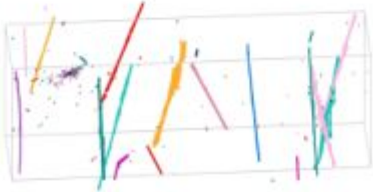

# Rejecting Random Coincident Cosmic-Ray Muons

**Through-going muon (TGM)**

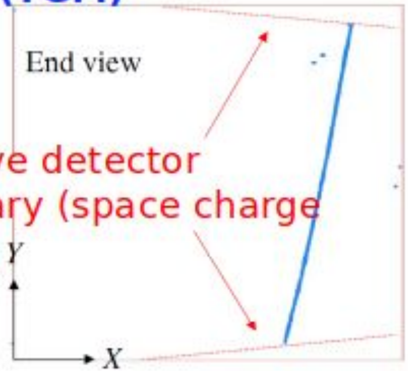


Effective detector boundary (space charge effect)

**Stopping muon (STM)**

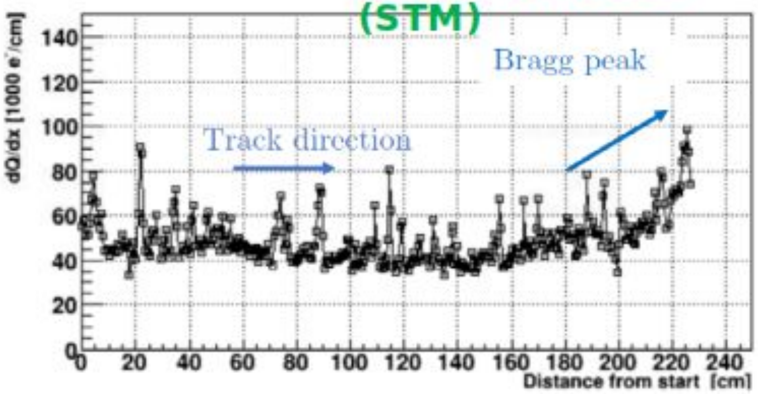


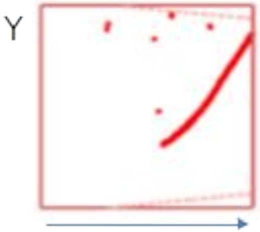


X (drift direction)

| | Neutrino:Cosmic-ray | |
|---|---|---|
| Charge-light matching | 1 : 6.4 | |
| TGM rejection | 1 : 0.91 | Improved by factor of >6 |
| STM rejection | 1 : 0.36 | Improved by factor of ~3 |
| Additional Cuts | 1 : 0.20 | |

# Wire-Cell 3D Pattern Recognition

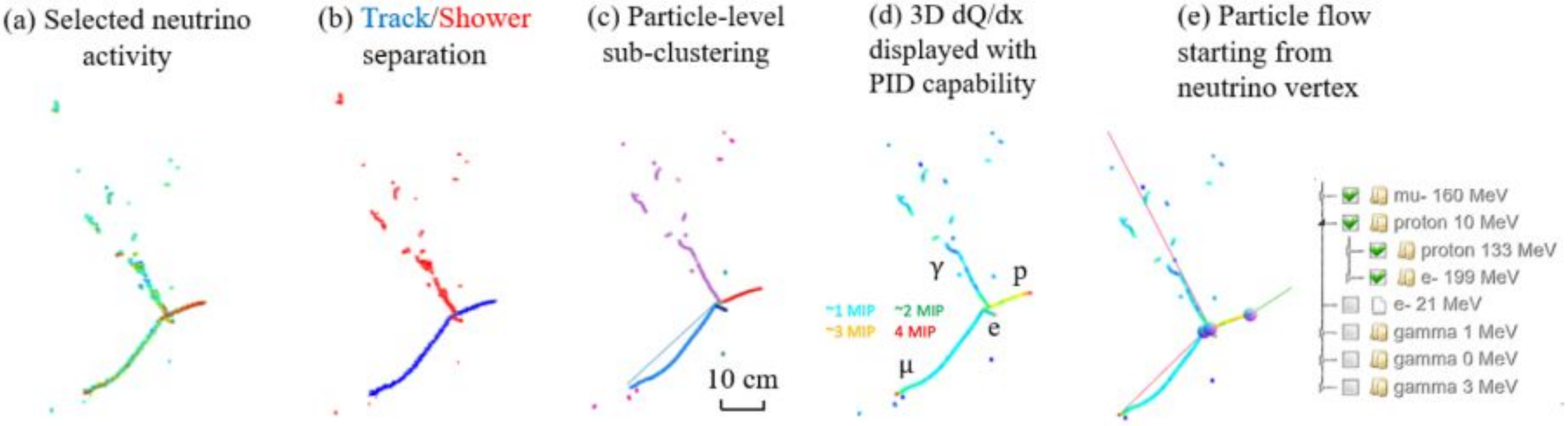


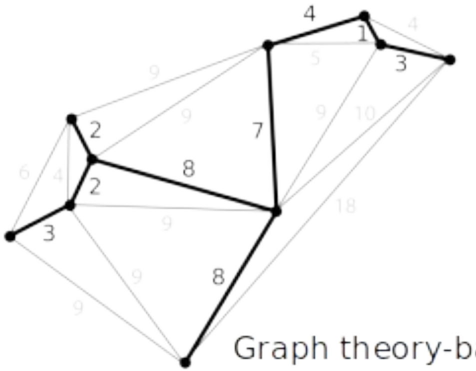

Graph theory-based multi-track fitting (e.g., Steiner tree)

**Hybrid of Traditional and Deep-Learning based approaches**

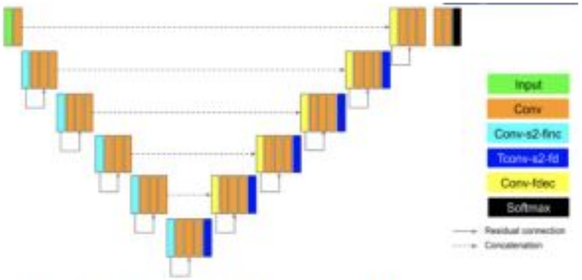


Deep-learning neural network for neutrino vertex identification

# CC Selection through XGBoost BDT


Human feature engineering

+

Machine learning algorithm:

XGBOOST: extreme Gradient Boosting

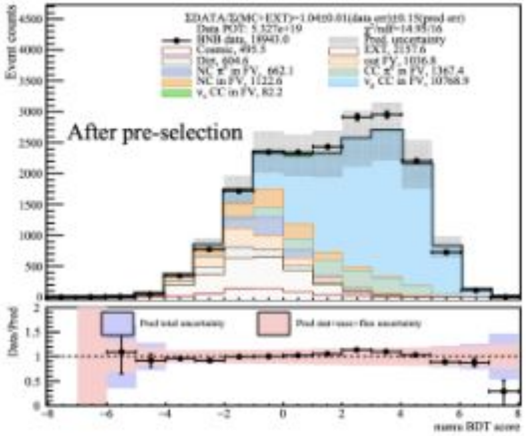


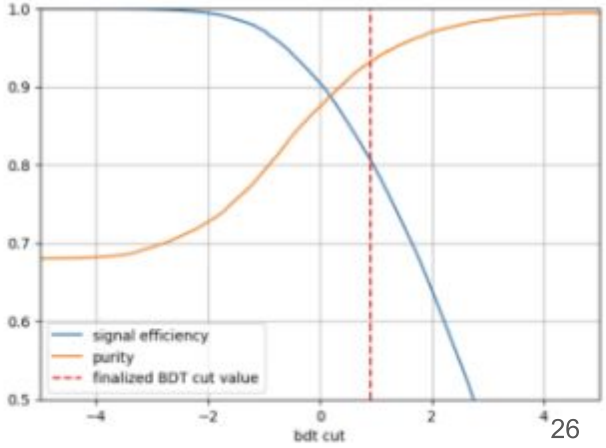

# How to estimate systematic uncertainties?

- Full systematic covariance

$$\Sigma^{syst} = \Sigma^{flux} + \Sigma^{xsec} + \Sigma^{det} + \dots$$


| | Multisim | Unisim |
|---|---|---|
| # of parameter variation at a time | Many | One |
| Parameter(s) variation | Random | Exactly 1 |
| # of MC run | One | Many (one per parameter) |
| Technical treatment | Event reweighting | Bootstrapping |

# Flux and cross section systematics: multisim

- Standard reweighting approach, each event has different weights from the randomization of the underlying model parameters.

| Tuning parameter name | Parameter type |
|---|---|
| $\pi^+$ hadron production | FLUX |
| $\pi^-$ hadron production | FLUX |
| $K^+$ hadron production | FLUX |
| $K^-$ hadron production | FLUX |
| $K^0_L$ hadron production | FLUX |
| horn current distribution | FLUX |
| horn current calibration | FLUX |
| nucleon total scattering Xs | FLUX |
| nucleon inelastic scattering Xs | FLUX |
| nucleon quasi-elastic scattering Xs | FLUX |
| pion total scattering Xs | FLUX |
| pion inelastic scattering Xs | FLUX |
| pion quasi-elastic scattering Xs | FLUX |
| MicroBooNE GENIE All | GENIE Xs ($\mu$B tune) |
| Strength of the CCQE RPA correction | GENIE Xs ($\mu$B tune) |
| Parameterization of the CCQE nucleon axial form factor | GENIE Xs |
| Parameterization of the CCQE nucleon vector form factors | GENIE Xs |
| Changes angular distribution of nucleon cluster in MEC | GENIE Xs ($\mu$B tune) |
| CCMEC Cross-section Shape | GENIE Xs ($\mu$B tune) |
| Angular distribution for RES $\Delta \to N + \pi$ | GENIE Xs |
| Angular distribution for RES $\Delta \to N + \gamma$ | GENIE Xs ($\mu$B tune) |
| Scaling factor for CC coherent $\pi$ production | GENIE Xs ($\mu$B tune) |
| Scaling factor for NC coherent $\pi$ production | GENIE Xs ($\mu$B tune) |
| Second-class vector current | Xs |
| Second-class axial current | Xs |
| $\pi^-$ interactions | GEANT4 |
| $\pi^+$ interactions | GEANT4 |
| proton interactions | GEANT4 |

Neutrino flux

Neutrino-argon cross section

Final-state hadron-argon interaction

*Geant4Reweight: JINST* 16 (2021) 08, P08042

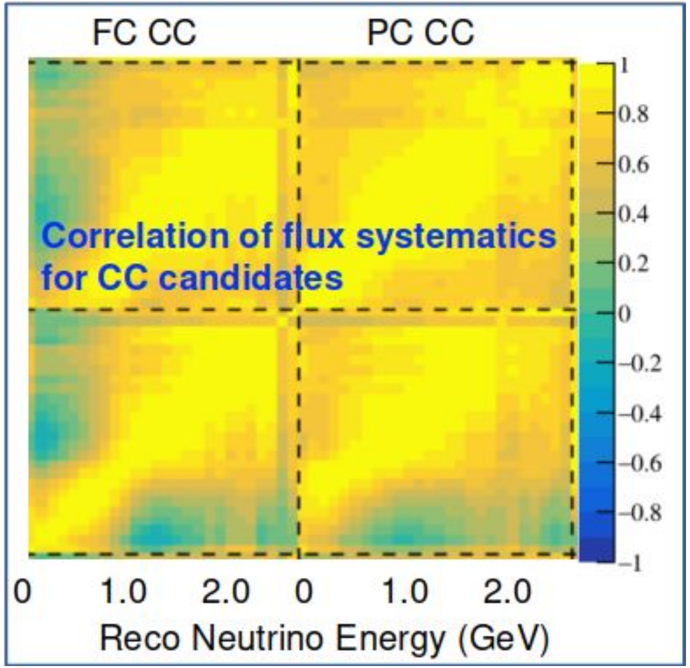

# Detector systematics: unisim

- Four major categories
  1) Light yield and propagation
  2) Charge readout detector response
  3) Recombination model ( to  conversion)
  4) Space charge effect (impacts on E-field)

- For each source of the systematic uncertainty, <u>the same set of MC simulation events are re-simulated</u> with a change to the detector modeling parameter of interest. In total, we have two samples
  1) One sample with nominal value of all parameters:
     <u>CV sample</u>
  2) One sample with changed value of interested par: <u>1σ sample</u>

Can not calculate the covariance matrix by the two samples in traditional way, which needs many samples with different pars values:

$$COV_{ij} = EXP\left[\left(X_i - \overline{X}\right)\left(X_j - \overline{X}\right)\right]$$

# Detector systematics: bootstrapping method

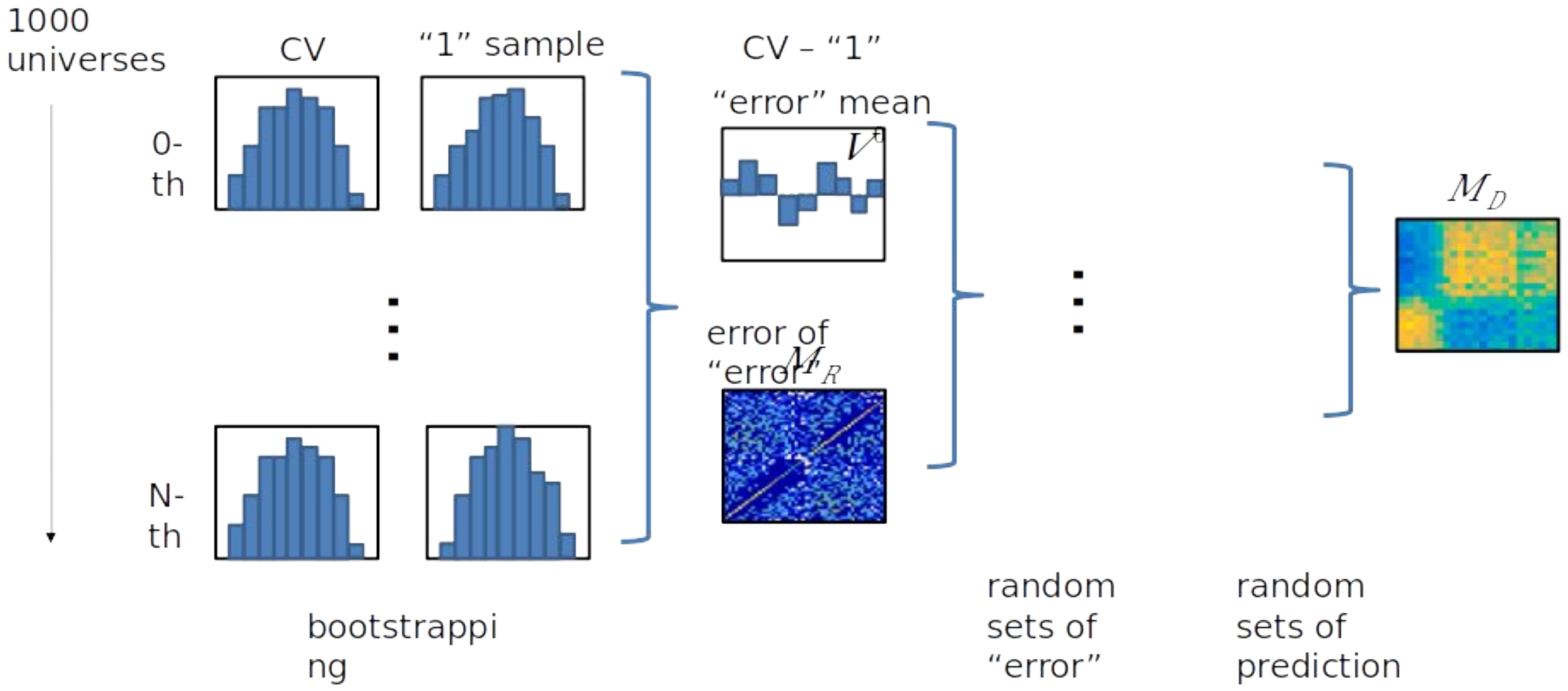

# Gaussian Processes Regression

$$\hat{\mu}_{a|b} = \mu_a + \Sigma_{K,ab}\Sigma_{T,bb}^{-1}(x_b - \mu_b)$$

Input bins b

$$\hat{\Sigma}_{T,a|b} = \Sigma_{K,aa} - \Sigma_{K,ab}\Sigma_{T,bb}^{-1}\Sigma_{K,ba}$$

Posterior bins a

$$\Sigma_K(x_1, x_2) = e^{-|(\vec{x}_1 - \vec{x}_2)\cdot\vec{s}|^2/2}$$

Inverse length scales s

# Testing Model Validation Procedure with Fake Data

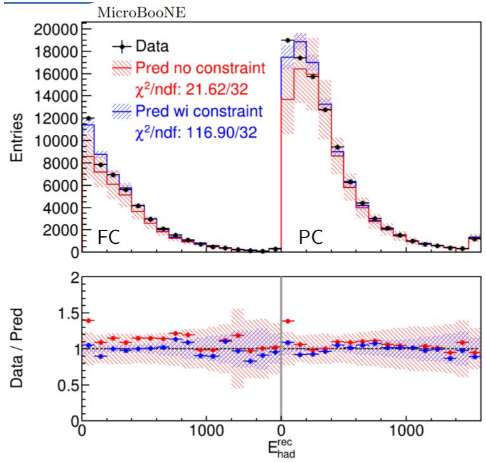


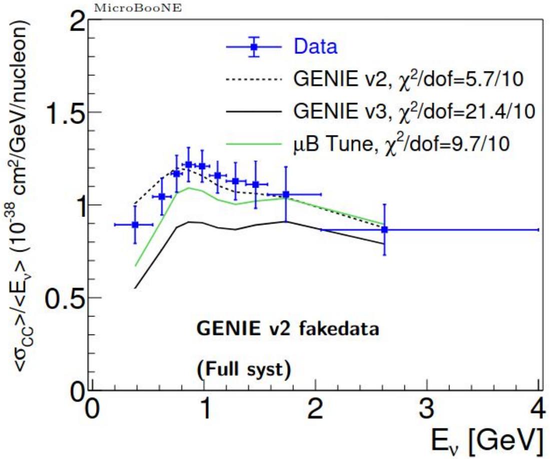


| Fake Data | GoF $\chi^2$/ndf | Unfolded XS w.r.t truth $\chi^2$/ndf | Type of Uncertainties Stat. + Syst. |
|---|---|---|---|
| **Genie v2** | **116.9/32** | **5.7/10** | **Fluctuations + Full** |
| **-15% $E_p$** | **39.5/16** | **4.1/10** | **Asimov + Xs only** |
| **-30% $E_p$** | **47.1/16** | **5.2/10** | **Asimov + Full** |

- Fake data generated from scratch with Genie v2 prediction
  - $7.2\times10^{20}$ POT exposure used
- Constrained model prediction fails validation test (**$\chi^2$/ndf = 116.9/32, p-value = $1.3\times10^{-11}$**) → $E_{had}^{missing}$ modeling disagreement
- Unfolded XS consistent with truth (**$\chi^2$/ndf = 5.7/10, p-value = 0.84** → Xs extraction is less sensitive to data/model discrepancy than the model validation)
  - Consistent with expectation
  - Similar observation in other fake data sets

# Equation For Unfolding

$$M_i - B_i = \sum_j R_{ij} \cdot S_j$$

$$\chi^2 = (\boldsymbol{M} - \boldsymbol{B} - \boldsymbol{R} \cdot \boldsymbol{S})^T \cdot \boldsymbol{V}^{-1} \cdot (\boldsymbol{M} - \boldsymbol{B} - \boldsymbol{R} \cdot \boldsymbol{S})$$

$$R_{ij} = \tilde{\Delta}_{ij} \cdot \tilde{F}_j$$

$$\tilde{\Delta}_{ij} = \frac{POT \cdot T \cdot \int_j F(E_{\nu j}) \cdot \sigma(E_{\nu j}) \cdot D(E_{\nu j}, E_{reci}) \cdot \varepsilon(E_{\nu j}, E_{reci}) \cdot dE_{\nu j}}{POT \cdot T \cdot \int_j F(E_{\nu j}) \cdot \sigma(E_{\nu j}) \cdot dE_{\nu j}}$$

➡ a MC ratio, less sensitive to Xs uncertainty

$$\tilde{F}_j = POT \cdot T \cdot \int_j \bar{F}(E_{\nu j}) \cdot dE_{\nu j}$$

$$S_j = \frac{\int_j \bar{F}(E_{\nu j}) \cdot \sigma(E_{\nu j}) \cdot dE_{\nu j}}{\int_j \bar{F}(E_{\nu j}) \cdot dE_{\nu j}}$$

} Not subject to prior knowledge of the Xs uncertainty

- ***V*** is the covariance matrix encoding:
  - Data statistical uncertainty: **M**
  - Flux uncertainty: **B, R (F)**
  - Cross-section (Xs) uncertainty: **B, R (σ)**
  - GEANT4 hadron interaction uncertainty: **B, R (D, ε)**
  - Detector-model uncertainty: **B, R (D, ε)**
  - "Dirt" uncertainty: **B**
  - POT uncertainty (2%): **M**
  - MC statistical uncertainty: **M**
- The unfolded cross section is defined based on the nominal flux
  - Easy for model comparisons
  - Simple for uncertainty calculation

PRD 102 (2020) 113012

# Equation For Unfolding

Measurements — Flux — Cross section — Detector response — Selection efficiency — Background

$$M(E_{rec}) = POT \cdot T \cdot \int F(E_\nu) \cdot \sigma(E_\nu) \cdot D(E_\nu \to E_{rec}) \cdot \varepsilon(E_\nu, E_{rec}) \cdot dE_\nu + B(E_{rec})$$

$$M_i = \sum_j R_{ij} \cdot S_j + B_i$$

$$\tilde{\Delta}_{ij} = \frac{POT \cdot T \cdot \int_j F(E_{\nu j}) \cdot \sigma(E_{\nu j}) \cdot D(E_{\nu j}, E_{rec i}) \cdot \varepsilon(E_{\nu j}, E_{rec i}) \cdot dE_{\nu j}}{POT \cdot T \cdot \int_j F(E_{\nu j}) \cdot \sigma(E_{\nu j}) \cdot dE_{\nu j}}$$

➡ a MC ratio, less sensitive to Xs uncertainty

$$R_{ij} = \tilde{\Delta}_{ij} \cdot \tilde{F}_j$$

$$\tilde{F}_j = POT \cdot T \cdot \int_j \bar{F}(E_{\nu j}) \cdot dE_{\nu j}$$

$$S_j = \frac{\int_j \bar{F}(E_{\nu j}) \cdot \sigma(E_{\nu j}) \cdot dE_{\nu j}}{\int_j \bar{F}(E_{\nu j}) \cdot dE_{\nu j}}$$

} Not subject to prior knowledge of the Xs uncertainty

| | GENIE 3.0.6 | NEUT 5.4.0.1 | NuWro 19.2.1 | GiBUU 2019.08 |
|---|---|---|---|---|
| Nuclear Model | LFG | LFG | LFG | LFG |
| QE | Valencia | Nieves | Lwlyn-Smith | standard |
| MEC | Valencia | Nieves | Nieves | empirical |
| Resonant | KLN-BS | Berger-Sehgal | Adler-Rarita-Schwinger | MAID (Spin-dependent) |
| Coherent | Berger-Sehgal | Rein-Sehgal | Berger-Sehgal | |
| FSI | hA2018 cascade | cascade | cascade | BUU transport model |

# Inclusive CC measurements

| Experiment | Target | References | Efficiency (%) | Purity (%) |
|---|---|---|---|---|
| **ArgoNeuT** | Ar | Phys. Rev. Lett. 108 161802<br>Phys. Rev. D 89 112003 | 49.5<br>42.0 (59.0) | 95<br>95.2 (91.2) |
| **MicroBooNE** | Ar | Phys. Rev. Lett. 123 131801<br>Phys. Rev. Lett. **128**, 151801 | 57.2<br>68 | 50.4<br>92 |
| **MINERvA** | CH, C/CH, Fe/CH, Pb/CH | Phys. Rev. Lett. 112, 231801<br>Phys. Rev. D94, 112007<br>Phys. Rev. Lett. 116 | 24 ~ 50 | 60 ~ 80 |
| **MINOS** | Fe | Phys. Rev. D81, 072002 | | |
| **NOMAD** | C | Phys. Lett. B660, 19 | 40.9 ~ 73.3 | 99.3 |
| **SciBooNE** | CH | Phys. Rev. D83, 12005 | 34.5 | ~90 |
| **T2K** | CH, $H_2O$, Fe | Phys. Rev. D87, 092003<br>Phys. Rev. D90, 052010<br>Phys. Rev. D93, 072002 | ~50<br>41.2<br>~50 @1GeV | ~86<br>89.4<br>~97 |